Journal of
MATERIALS RESEARCH

Probing of microvoids in high-rate deposited *a*-Si : H thin films by variable energy positron annihilation spectroscopy

X. Zou, D. P. Webb, Y. C. Chan, and Y. W. Lam
Department of Electronic Engineering, City University of Hong Kong, Tat Chee Avenue, Kowloon, Hong Kong

Y. F. Hu, S. Fung, and C. D. Beling
Department of Physics, The University of Hong Kong, Pokfulam Road, Hong Kong

(Received 15 May 1997; accepted 13 January 1998)

In this paper, positron annihilation measurements have been carried out on *a*-Si : H thin films deposited by plasma-enhanced chemical vapor deposition (PECVD) at high and low rates by means of the variable energy positron beam Doppler-broadening technique. The depth profiles of microvoids in the films grown under different conditions have been determined. We found a smaller void fraction in the surface region of all films compared to the bulk, and a smaller void fraction in low rate than in high growth rate films. By plotting S and W parameters in the (S, W) plane, we have shown that the vacancies in all of the high-rate and low-rate deposited intrinsic samples, and in differently doped low-rate samples are of the same nature, although there appears to be a higher density of defects in the boron than phosphorus doped films. The depth profiles of the microvoid-like defects in the *a*-Si : H films are extracted by use of the VEPFIT program.

I. INTRODUCTION

Amorphous tetrahedral semiconductors are important materials for the fabrication of micro- and optoelectronic devices. Advances in this area have, however, been hindered by the limited understanding of their structure, and thus electronic properties, even at the most elementary level. For instance, light-induced degradation of hydrogenated amorphous silicon alloy materials and devices has been the subject of intensive studies, but the origin of the metastability has not been unambiguously identified, and the list of causes includes hydrogen, impurities like C, O, or N, microvoids due to inhomogeneous growth, weak bonds, or a combination of these. Microvoids have also been suggested as metastability centers in *a*-Si : H, especially in high-rate deposited *a*-Si : H thin film. Therefore, attention should be focused on microvoid characterization.

Using the small-angle x-ray scattering (SAXS) measurement, it has been demonstrated[1,2] that even in the best quality material, microvoids of typical diameter 1.0 nm exist, occupying a volume fraction of about 1%. The void density is typically larger for poorer quality material.[3] A correlation between the microvoid density in the material with the initial and light-degraded performance of solar cells in which the intrinsic layer has varying microvoid densities caused by changes in the deposition rate has also been established.[4]

Most defect characterization techniques are not sensitive enough to measure small quantities of point defects generated during thin film growth. However, the newly emerging technique, variable energy positron annihilation spectroscopy (VEPAS), is highly sensitive to vacancy-type defects in thin films and has been very successfully used to reveal the presence of vacancy-like defects such as small clusters or vacancy-impurity complexes.[5] Theoretical calculations of the annihilation characteristics and positron states for defects also play a very important role as regards achieving the correct interpretation of the experimental results, and they are crucial when one is dealing with very complex materials.[6] Positron annihilation is thus expected to become an increasingly powerful tool for identifying defects present in solid state materials.

One of the most widely adopted research areas for positrons has been the identification and study of various types and concentrations of defects in solids,[7] in particular, defect properties at and near the surfaces of the materials characterized.[8] One of the most striking advantages of the positron beam technique follows from the narrow energy width and controllable energy making possible nondestructive measurements of the surfaces, interfaces, and thin films. Moreover, valuable information on a greater variety of defect-related problems is obtained that can not be supplied by other surface sensitive spectroscopies.

Point defects can be probed with positron annihilation spectroscopy at a level (10^{-7} atomic fraction) inaccessible to conventional techniques. Since *a*-Si : H

contains numerous structural defects and impurities such as hydrogen and dopant ions, these materials provide a rich environment for positron study, yet there have been few such studies to date.

Annihilation of positrons from defect states gives rise to the observables routinely used in PAS; they include the Doppler broadening spectrum indicating line-shape parameters S and W of γ-ray emission resulting from annihilation of positrons with electrons, angular correlation spectrum, lifetime, centroid shift, and positronium fraction.

Extant positron annihilation studies on *a*-Si : H have utilized lifetime spectroscopy measurements made with the energetic positrons of ^{22}Na decay. Positron lifetimes in *a*-Si : H films produced by evaporation and by sputtering were measured by Dannefaer *et al.*[9] They found that both types of film contained void-like defects, with sizes estimated to be the equivalent of about five vacancies from comparison of the lifetime components to those for vacancy clusters in crystalline Si. A comparison of RF-sputtered *a*-Si and *a*-Si : H to crystalline Si by Jung *et al.*[10,11] showed that both *a*-Si and *a*-Si : H had a long lifetime component ($\approx$400 ps) characteristic of microvoids. This, however, was assigned to a void size smaller than four missing atoms. The *a*-Si : H was found to have a smaller concentration of these defects, as indicated by a lower intensity of the 400 ps component. Similar lifetime studies were conducted by Schäefer *et al.*[12] However, the interpretation of the size of the vacancies remains in dispute.[13,14]

With regard to depth resolved studies employing variable energy positron beams, Leo *et al.* measured Doppler broadening from *a*-Si and *a*-Si : H thin films relative to crystalline Si using a positron source and without attempting depth resolution.[15] Harkvoort *et al.* studied three types of *a*-Si, namely: CVD-prepared, sputter deposited from a Kr plasma, and Si^+ ion beam amorphized, and found fitted annihilation radiation line-shapes (S values) and positron diffusion lengths for the amorphous layers that showed large variations with the processing steps and subsequent annealing.[16] On average, *a*-Si was found to produce S values greater than those observed for divacancies and microvoids in crystalline Si. Apart from these studies there have been few reports of attempts to depth profile and characterize the microvoids in *a*-Si : H using VEPAS.

In this paper, we report on a VEPAS investigation on *a*-Si : H thin films deposited at a high deposition rate of over 1.5 nm/s, producing information on the depth profile, nature, and concentration of microvoids. The paper is arranged as follows: in Sec. II we present experimental details of sample preparation and positron annihilation measurements. The experimental results and discussion are, respectively, presented in Secs. III and IV and conclusions are drawn in the final section.

II. EXPERIMENTAL DETAILS

A. Sample descriptions

The samples in this work were $1-2$ μm intrinsic *a*-Si : H thin homogenous films grown by pure silane (SiH_4) RF glow discharge plasma-enhanced chemical vapor deposition (PECVD) at a deposition rate of 1.5 nm/s[17] on quartz substrates, and $1-2$ μm *p*- and *n*-type *a*-Si : H films deposited by glow discharge using gas mixtures of ($SiH_4 + B_2H_6 + H_2$) and ($SiH_4 + PH_3 + H_2$), respectively, at a deposition rate of 0.2 nm/s on quartz substrates. For both types of dopant the gas ratio was about 7×10^{-3}. The rf power was varied between 8 and 40 W, and the substrate temperature varied between 280 °C and 330 °C. The quality of the thin films was evaluated by photoconductivity measurements. The ratio of photoconductivity and dark-conductivity of the intrinsic films is about 5 orders, and the magnitude of conductivity of *p*- and *n*-type *a*-Si : H are $10^{-2}\Omega^{-1}$ cm^{-1} and $10^{-1}\Omega^{-1}$ cm^{-1}, respectively. The samples are listed in the caption to Table I.

During the preparation of the films, a mass spectrometer was used to monitor the concentration of SiH_n^+ radicals.

TABLE I. Summary of fitted values of upper boundaries of chosen regions, S values, and effective positron diffusion length $L_{+,\mathrm{eff}}$, derived, using a 3-layered model, from measured S parameters for high growth rate undoped, low-rate deposited *p*-doped and *n*-doped *a*-Si : H thin films. (A) undoped, RF = 40 W, T_s = 330 °C. (B) undoped, RF = 20 W, T_s = 300 °C. (C) *p*-doped, RF = 20 W, T_s = 280 °C. (D) *p*-doped, RF = 8 W, T_s = 280 °C. (E) *n*-doped, RF = 20 W, T_s = 280 °C. (F) *n*-doped, RF = 8 W, T_s = 280 °C.

Samples	A (undoped)	B (undoped)	C (*p*-doped)	D (*p*-doped)	E (*n*-doped)	F (*n*-doped)
x_1 (nm)	5.1	13.6	13.0	14.6	22.1	7.6
x_2 (nm)	1600.3	1857.4	1725.4	1512.3	1410.3	1904.0
S_s	0.5729	0.5835	0.5284	0.4987	0.5099	0.4670
S_f	0.5826	0.5825	0.5798	0.5609	0.5770	0.4798
$L^s_{+,\mathrm{eff}}$ (nm)	18.7	17.2	19.3	29.5	24.1	30.5
$L^f_{+,\mathrm{eff}}$ (nm)	10.6	10.9	13.7	22.2	13.0	25.6

B. Variable energy positron annihilation spectroscopy

The positron beam annihilation experiments were performed using a mono-energetic positron beam of intensity 5×10^4 e^+s^{-1} over an energy range from 0.15 to 25 keV in steps of 250 eV, details of which have reported elsewhere.[18] In the experimental setup, positrons radiated by a $^{22}Na\beta^+$ source are implanted in the W foil transmission moderator. After thermalization and then diffusion, positrons possessing small energy are accelerated by a magnetic field, to form a positron beam with a certain monoenergy. The variation of beam energy allows control over the mean depth of positron implantation into the samples, although the depth distribution of the thermalized positrons is broad and asymmetric, extending to about twice the mean depth. In general, the mean penetration depth of the positrons implanted at energy E can be determined from the following power law

$$x_0 = AE^n, \tag{1}$$

where the constant A in Eq. (1) has been found empirically to be $A \sim 400/\rho$ $\text{Å}/(\text{keV})^n$, ρ being the sample density in g/cm^3, x_0 is in Å, E is in keV, and the power $n \approx 1.6$ for most materials.[19,21] Thus for *a*-Si : H ($\rho = 2.2$ g cm^{-3}) the maximum positron beam energy 25 keV employed in the present study corresponds to a mean positron stopping depth of about 3 μm. This energy range was chosen so that at a certain positron implantation energies all positrons essentially annihilate in the *a*-Si : H film, while at the highest energies almost full penetration into the quartz substrate could be achieved; thus depth profiling may be performed across the entire *a*-Si : H film.

The 511 keV annihilation γ radiation from the sample was detected with a high purity Ge detector of resolution 1.4 keV at 514 keV and a digitally stabilized multichannel analyzer system. A total of 1×10^6 counts were collected under the annihilation photopeak of γ-rays for each positron energy. The photopeak line shape of γ-rays was described using the conventional valence and core annihilation parameters S and W, which are the ratios of counts in the central and wing portions of the annihilation photopeak to the total counts in the peak, respectively.[5] The energy windows were set so that the S parameter represented the fraction of positrons annihilating mainly with valence electrons having a longitudinal momentum component of $p_L \leqslant 3.7 \times 10^{-3}\ m_0c$, where m_0 is the electron mass and c the speed of light. The W parameter, representing the fraction of annihilations with the core electrons, was set over the larger momentum component range of $11 \times 10^{-3}\ m_0c \leqslant p_L \leqslant 29 \times 10^{-3}\ m_0c$.

III. RESULTS AND ANALYSIS

Positrons get trapped at neutral and negative vacancy defects because the missing positive charge of the ion cores causes the particle to experience a potential well. The reduced valence and core electron density at a vacancy increases the lifetime of the trapped positron and moreover narrows the positron momentum distribution since the relative proportion of valence to core annihilations increases. Consequently, with increasing number of microvoids, the valence annihilation parameter S increases and the core annihilation parameter W decreases. The momentum distribution of the annihilated core electrons contains information on the atomic numbers of ions. A trapped positron at a vacancy overlaps mainly with the core electrons of the nearest neighbor atoms. Hence, the shape and magnitude of the core electron momentum distribution can be used to identify the nature of the vacancy acting as a positron trap.

A. Positron implantation and diffusion in *a*-Si : H thin films

After thermalization, i.e., after the positrons have been implanted with profile $P(x, E)$ and have been slowed down to thermal energies, they can still propagate some distance through the sample before they are annihilated. The positrons diffuse in the sample with diffusion constants governed by the nature and quality of the material layer until eventually they annihilate with electrons.

Positron motion in the absence of an electric field is well described by the one-dimensional diffusion annihilation equation[20]

$$D_+\nabla^2 n(x,E) - [\lambda_b + \mu C_{\text{vac}}(x)]n(x,E) + P(x,E) = 0, \tag{2}$$

where D_+ is the position diffusion coefficient, $n(x, E)$ the quasistationary positron density at the depth x for the incident positron energy E, λ_b the free-positron annihilation rate, μ the specific trapping rate by vacancies, C_{vac} the vacancy concentration, and $P(x, E)$ the positron implantation profile. The form of the implantation profile is to a good approximation the derivative of a Gaussian[21]

$$P(x,E) = \left(\frac{2x}{x_0^2}\right)e^{-(x/x_0)^2}, \tag{3}$$

where x_0 is given by expression (1), and this form has been used in the present work.

Solution of Eq. (2) for arbitrary $P(x, E)$ leads to the definition of the effective positron diffusion-length which can be represented as[5]

$$L_{+,\text{eff}} = \left(\frac{D_+}{\lambda}\right)^{1/2} = \left(\frac{D_+}{\lambda_b + \mu C_{\text{vac}}}\right)^{1/2}. \tag{4}$$

Assuming a uniform defect profile in an *a*-Si:H thin film, the positron trapping rate in the defects is related to the effective positron diffusion length by

$$\mu C_{\mathrm{vac}} = \frac{D_+}{L_{+,\mathrm{eff}}^2} - \lambda_b , \qquad (5)$$

which is a useful equation for evaluating the density of defects in *a*-Si : H, since $L_{+,\mathrm{eff}}$ can be experimentally determined. To accomplish this, the *S* parameter versus energy data are analyzed using the program VEPFIT,[22] which solves the diffusion annihilation Eq. (2) for positrons in the *a*-Si : H thin film structure, including the effects of defects. In this study, VEPFIT calculates, for each incident positron beam energy *E*, the fractions of positrons which annihilate in the surface region of *a*-Si : H thin film $F_s(E)$, which annihilate in the bulk of *a*-Si : H thin film $F_f(E)$, and which annihilate in the quartz substrate $F_q(E)$, for each sample. The experimental lineshape parameter $S(E)$ can then be fitted to obtain the characteristic *S* value for each region, using the equation

$$S(E) = F_s(E)S_s + F_f(E)S_f + F_q(E)S_q , \qquad (6)$$

where the subscripts *s*, *f*, and *q* refer to the *a*-Si : H surface and bulk, and the quartz substrate, respectively.

The fitting performed by VEPFIT gives the effective diffusion length $L_{+,\mathrm{eff}}$ for the *a*-Si : H thin film together with values for S_s, S_f, and S_q. Of these three *S* parameters only S_f is expected to reveal the degree of microvoid trapping in the *a*-Si : H thin film. Table I summarizes the fitted results for undoped, *p*-doped, and *n*-doped thin films.

B. Microvoids at surface region in high-rate deposited *a*-Si : H

Figure 1 shows the positron lineshape parameter *S* measured versus incident energy for *a*-Si : H thin films prepared under different process conditions. The same general trend is observed in both samples. The results clearly demonstrate that there is a depth variation in microvoid volume fraction. A deposition condition dependency can also be seen.

The *S* parameters vary from about 0.565 to 0.579 at low positron implanting energy. This is attributed to positrons annihilating within the surface region. As the implanting energy increases, more positrons annihilate in the bulk of *a*-Si : H, and this results in an increase of the *S* parameter to a value of about 0.583, which may be identified as the characteristic value of the *a*-Si : H. The *S* parameter decreases with further increase in positron implanting energy as more positrons annihilate in the quartz substrate and thus finally approaches the same value characteristic of bulk quartz for all samples.

It can be easily seen that for high-rate deposited *a*-Si : H thin films with different rf power and substrate

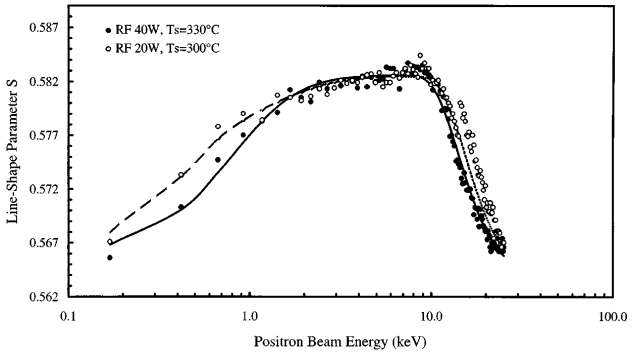

FIG. 1. Doppler-broadening lineshape parameter *S* as a function of incident positron energy for high-rate deposited *a*-Si : H thin film with different RF power and substrate temperature. The filled circle is for RF power of 40 W and substrate temperature of 330 °C (sample A), and the open circles for RF power of 20 W and substrate temperature of 300 °C (sample B). Solid and dash lines show VEPFIT fits to the data.

temperature, the microvoid profile appears the same in the bulk, but obvious differences exist in the surface region for positron beam incident energy below 1 keV, corresponding to about 180 Å according to Eq. (1). It seems that higher rf power coupled with higher substrate temperature is of benefit in eliminating microvoids within the surface region of high-rate deposited *a*-Si : H. This is mainly due to the relative concentrations of monosilicon radicals when the rf glow discharge is off. The relevant reactions are as follows:

$$e^- + \mathrm{SiH_4} \longrightarrow \mathrm{SiH_2} + \mathrm{H_2} + \mathrm{e}^- \quad 2.2\ \mathrm{eV}, \qquad (7a)$$

$$e^- + \mathrm{SiH_4} \longrightarrow \mathrm{SiH_3} + \mathrm{H} + e^- \quad 4.0\ \mathrm{eV}, \qquad (7b)$$

$$e^- + \mathrm{SiH_4} \longrightarrow \mathrm{Si} + 2\mathrm{H_2} + e^- \quad 4.2\ \mathrm{eV}, \qquad (7c)$$

$$e^- + \mathrm{SiH_4} \longrightarrow \mathrm{SiH} + \mathrm{H_2} + \mathrm{H} + \mathrm{e}^- \quad 5.7\ \mathrm{eV}. \qquad (7d)$$

The corresponding electron threshold energies are as labeled. As is well known, the number of vacancies is tightly correlated with the SiH_2 density in the plasma.[23] At higher rf power, the reaction process described by (7b), (7c), and (7d) will dominate the glow discharge and amounts of radical SiH_2 will decrease, which is conducive to eliminating microvoids within the surface region of high growth rate *a*-Si : H by PECVD.

The density of microvoids in *a*-Si : H can be found using Eq. (5). The effective diffusion length of positrons in the surface region and in the bulk of *a*-Si : H were found to be, by VEPFIT, 18.7 nm and 10.6 nm for 40 W deposited and 17.2 nm and 10.9 nm for 20 W deposited *a*-Si : H thin film. Adopting as the value for the specific positron trapping rate for vacancy defects to be that in crystalline Si,[24] $\mu = 3 \times 10^{14}\ \mathrm{s}^{-1}$, we derived defect concentrations from the *S*-parameter data of 2.1×10^{-3} atomic fraction (at. fr.) in the surface region and 6.5×10^{-3} at. fr. in the bulk for the 40 W, and 2.5×10^{-3} at. fr. in the surface region and 6.2×10^{-3} at. fr. in the

bulk for the 20 W deposited sample. Again using *c*-Si data, the diffusion coefficient of positrons was taken as $D = 2.2\ \mathrm{cm}^2/\mathrm{s}$. The annihilation rate, corresponding to *c*-Si divacancies, was taken as $\lambda_b = 4.59 \times 10^9\ \mathrm{s}^{-1}$.[25] These evaluated results clearly demonstrate the effect of rf power on the production of microvoids in the near surface region of *a*-Si : H thin film.

C. Deposition rate effects on microvoid concentration

Low growth rate *a*-Si : H thin films exhibit fewer microvoids both within the surface region and in the bulk compared to high growth rate films, which can be seen from the comparison in Fig. 2. The diffusion lengths of positrons $L^s_{+,\mathrm{eff}}$ in the surface region and $L^f_{+,\mathrm{eff}}$ in the bulk of *a*-Si : H obtained from VEPFIT fitting of the *S* parameter were 18.7 nm and 10.6 nm, respectively, for high growth rate *a*-Si : H giving defect densities of 2.1×10^{-3} at. fr. and 6.5×10^{-3} at. fr., respectively, and 24.1 nm and 13.0 nm for low growth rate *a*-Si : H, respectively, giving defect densities of 1.2×10^{-3} at. fr. and 4.3×10^{-3} at. fr., respectively.

A clear correlation between microvoid fraction and deposition process conditions is apparent. As the deposition rate of the low rate process is about 0.2 nm/s, which was carried out by hydrogen-diluted silane glow discharge with rf power of 8 W, the dominant process should be that as described by (7b) because of the hydrogen depression of reaction (7a). Therefore, the monosilicon radical SiH_3 is in the majority in the low-rate PECVD process in this work, and consequently fewer microvoids exist in the low growth rate *a*-Si : H than in the high-rate deposited *a*-Si : H.

D. Effects of doping species on microvoid concentration

Preliminary studies on the effect of the dopant on microvoid concentration was also carried out in this work, and the plots of *S*-parameter variation against energy for *p*- and *n*-type *a*-Si : H are illustrated in Fig. 3. Fitting results yield surface and bulk diffusion lengths of 29.5 nm and 22.2 nm for *p*-type *a*-Si : H and 30.5 nm and 25.6 nm for *n*-type *a*-Si : H, and consequently defects densities in the surface region and the bulk region can be derived as 8.3×10^{-4} at. fr. and 1.5×10^{-3} at. fr. for *p*-type and 7.7×10^{-4} at. fr. and 1.1×10^{-3} at. fr. for *n*-type *a*-Si : H. These results indicate that the boron dopant induces more microvoids than the phosphorous dopant. It is noteworthy that boron doping is also more difficult and less efficient than phosphorous doping. Evidently the increased microvoid fraction reflects the greater difficulty of accommodating boron in the silicon network. Further VEPAS studies on varying doping *a*-Si : H thin films are in hand to elucidate this point, the results of which will be published in the future.

IV. DISCUSSION

A. Identification of microvoid nature in both high-rate and low growth rate *a*-Si : H

In principle, an increase in *S* can be induced by either an increase in the concentration or a change in the nature of trapping sites. Information concerning the type of trapping center can be obtained by deducing a defect-specific parameter on the basis of a two-state trapping model. If S_b and S_v are the characteristic values of the lineshape parameter *S* for positrons annihilating when free and when trapped, respectively, then

$$S = F_b S_b + F_v S_v , \tag{8}$$

where F_b and F_v are the relative probabilities of each kind of annihilation event. F_v is given by

$$F_v = \frac{\mu C_{\mathrm{vac}}}{\lambda_b + \mu C_{\mathrm{vac}}} , \tag{9}$$

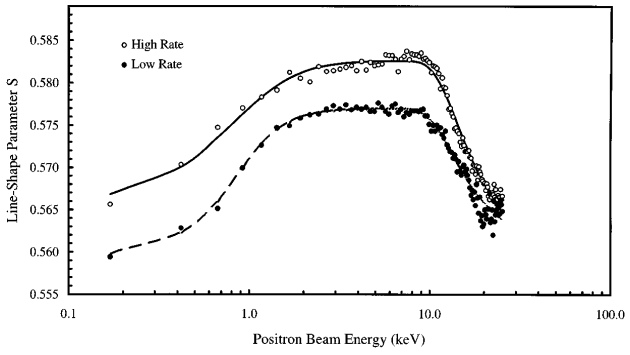

FIG. 2. Comparison of *S* parameters between high and low growth rate *a*-Si : H. The filled circle is for a deposition rate of 0.2 nm/s (sample F), and the open circle for a deposition rate of 1.5 nm/s (sample A). The lines show VEPFIT fits.

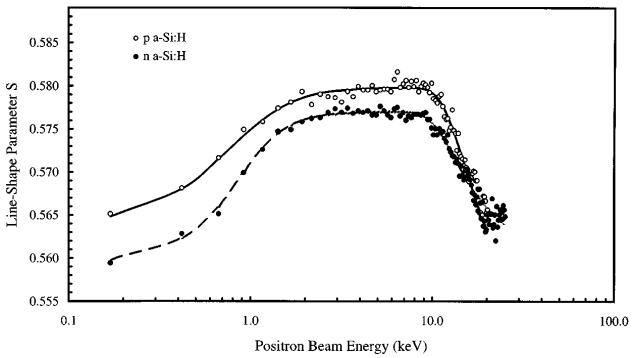

FIG. 3. Dopant effect on *S*-parameters of *a*-Si : H. Both *p*- and *n*-type *a*-Si : H have been prepared under RF power of 8 W and substrate temperature of 280 °C. The lines show VEPFIT fits.

in which the parameters are as defined previously. If one substitutes Eq. (9) into Eq. (8), and using $F_b + F_v = 1$, one can find that

$$S = \left(1 - \frac{\mu C_{\text{vac}}}{\lambda_b + \mu C_{\text{vac}}}\right) S_b + \frac{\mu C_{\text{vac}}}{\lambda_b + \mu C_{\text{vac}}} S_v . \quad (10)$$

An equivalent relation can be deduced for the line-shape wing parameter W. Then the changes in the two parameters due to trapping can be written as

$$S - S_b = \frac{\mu C_{\text{vac}}}{\lambda_b + \mu C_{\text{vac}}} (S_v - S_b) , \quad (11)$$

$$W - W_b = \frac{\mu C_{\text{vac}}}{\lambda_b + \mu C_{\text{vac}}} (W_v - W_b) , \quad (12)$$

The differences $S - S_b$, $W - W_b$, still depend on defect concentration. A concentration independent characteristic parameter R was defined by Mantl and Triftschäuser[26,27] to be

$$R = \left| \frac{S - S_b}{W - W_b} \right| = \left| \frac{S_v - S_b}{W_v - W_b} \right| . \quad (13)$$

The definition assumes only one type of trapping center is present. If several types of trapping sites are available to the positrons at the same time, R is valid as long as one type predominates.[26,27]

Therefore, the number of different vacancy-type positron traps in *a*-Si : H can be identified by investigating the linearity between the valence and core annihilation parameters.[28] As indicated above, if only a single type of vacancy defect is present, the W parameter depends linearly on the S parameter. The inverse slope of a straight line fit of the W-S plot is the defect characteristic parameter R, as shown by Eq. (13). This analysis is represented in Fig. 4 by plotting the W parameter as a function of the S parameter for VEPAS scans of a number of *a*-Si : H samples formed under different processing.

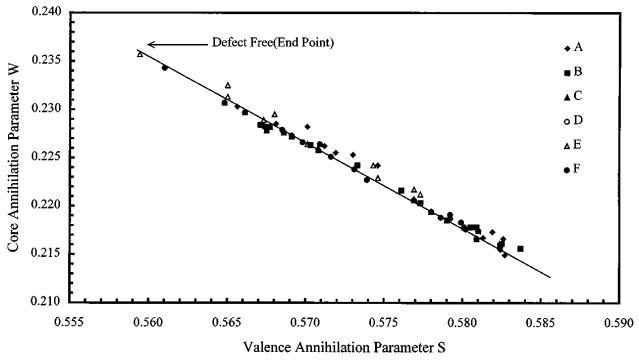

FIG. 4. The core annihilation parameter W versus the valence annihilation parameter S, in all of the high and low growth rate, doped and undoped, *a*-Si : H thin films. The annihilation parameters in defect-free thin films are indicated. The statistical errors of the S and W parameters are $\sigma_s = 0.0004$ and $\sigma_w = 0.0004$.

It is noted in Fig. 4 that the data from all of the samples, high rate, low rate, and doped, are plotted on the same graph. Despite the variations in deposition conditions, it can be seen that all the data points fall on the same line in the W-S plane, indicating that vacancy type in all samples is the same. The characteristic value of this vacancy is the inverse slope, $R = |\Delta S/\Delta W| \approx 1.2$, of the straight line in Fig. 4.

The straight line in the (S, W) plane is formed between the end points (S_b, W_b) and (S_v, W_v) corresponding to the delocalized positron state in the bulk and the localized state at the microvoid, respectively. When different types of vacancies exist in the same material, all the straight lines in the (S, W) plane have the same end point at (S_b, W_b). The end point in Fig. 4 is thus an upper limit for the annihilation parameters of the delocalized positron in defect-free *a*-Si : H thin film, which values are $(S_b, W_b) = (0.559, 0.236)$.

The maximum change of the annihilation parameters S and W compared to the end point (S_b, W_b) gives information on the nature of the detected microvoid defects. Summarized in Table II are the maximum S/S_b and W/W_b ratios for each samples. These values do not vary much among the samples, and thus we may conclude they are characteristic of the defect type.

B. Depth profile of defect density in *a*-Si : H

Equation (5) shows that the position dependent diffusion length $L(x)$ is a primary source of information about the defect concentration profile $C_{\text{vac}}(x)$ in an *a*-Si : H thin film. To obtain the depth variation of positron diffusion length L, a multilayer model with a sufficient number of layers should be used in the VEPFIT fitting.

To fit the S-parameter profiles, a five-layered model, consisting of surface layer (*a*-Si : H)/three bulk layers (*a*-Si : H)/quartz substrate, was adopted. Figure 5 compares the S curve corresponding to the parameters found by the fit for a high rate sample, sample B deposited under 20 W and 300 °C, and Fig. 6 the corresponding depth $L_{+,\text{eff}}$ and defect concentration profiles. A clear variation at the interface between the surface layer (~13 nm) and the bulk layer can be seen from the figure, and a drastic change in defect concentration exists at the initially grown layer (~1000 nm, corresponding to the thickness of *a*-Si : H film). The rise in microvoid concentration at the interface indicates that the structure of the *a*-Si : H thin film takes a few atomic layers to stabilize as a result of lattice mismatch, which is an implication of the interface effects possibly caused by the mismatch between the networks of *a*-Si : H thin film and quartz substrate.

TABLE II. Summary of maximum change of annihilation parameters S and W.

Samples	A (undoped)	B (undoped)	C (p-doped)	D (p-doped)	E (n-doped)	F (n-doped)
Max. S/S_b	1.044	1.045	1.041	1.041	1.033	1.040
Max. W/W_b	0.976	0.971	0.980	0.980	0.998	0.993

As illustrated in Figs. 5 and 6, a similar trend of S-E and C_{vac}-x plots is shown. In the earlier part of this paper, it was revealed that the microvoid defects in a-Si : H thin film are of uniform nature; this implies that the variation, increase or decrease, in S parameter is caused by the variation, increase or decrease, in defect concentration in a-Si : H.

V. CONCLUSIONS

In summary, we have carried out positron annihilation measurements on high-rate and low-rate a-Si : H thin films deposited by PECVD. By means of the slow positron beam Doppler-broadening technique, the depth profiles of microvoids in the films have been resolved. It was found that there is a smaller void fraction in the surface layer, to a depth of appropriately 18 nm, than in the bulk. The boron doped showed a greater bulk void fraction than phosphorous doped films. By plotting S and W parameters in the (S, W) plane, we have found that the microvoids in all of the high-rate and low-rate deposited intrinsic, and low rate doped a-Si : H films are of the same nature. The depth profile of defect concentrations in a-Si : H were extracted by VEPFIT fitting, which indicated an approximately uniform density of defects throughout the thin films, but with an enhanced concentration at both the near surface region and the substrate interface due to network mismatch. This implies that the similar trend between S-E and C_{vac} plots is predominantly caused by concentrations of the vacancy-like defects in a-Si : H.

We would like to point out that although we see a correlation between deposition conditions and the concentration of microvoids in all differently processed samples, these results should be considered only to depict the trend under certain deposition parameters. To conclude, we have demonstrated that positron annihilation is a powerful technique to characterize vacancy-type defects in a-Si : H, especially to give a depth profile of such defects. This capability we intend to apply in future for the characterization of multilayered thin film structures. Positron annihilation may prove to be a useful tool for the optimization of interfaces in order to improve the performance of multilayer devices.

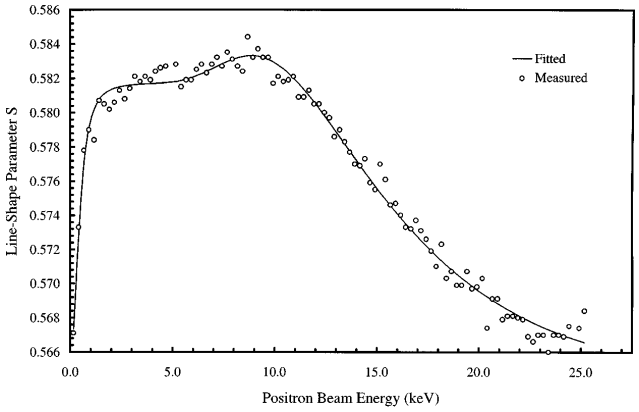

FIG. 5. Five-layered VEPFIT fitted results, illustrated by a solid line, compared with measured S-parameter data, as a function of positron beam incident energy E. The specimen used in the measurement is of the high growth rate type with a deposition rate of 1.5 nm/s, under RF = 20 W, T_s = 300 °C (sample B).

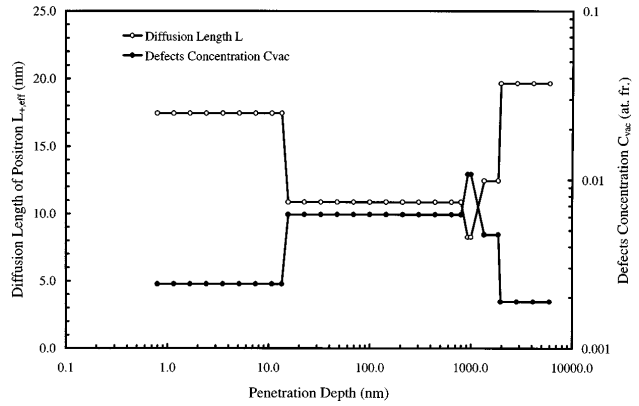

FIG. 6. The position dependent effective diffusion length $L_{+,\text{eff}}$ and the depth profile of defects concentration versus positron penetration depth, extracted from the fit shown in Fig. 5.

REFERENCES

1. D. L. Williamson, A. H. Mahan, B. P. Nelson, and R. S. Crandall, J. Non-Cryst. Solids **114**, 226 (1989).
2. A. H. Mahan, D. L. Williamson, B. P. Nelson, and R. S. Crandall, Phys. Rev. B **40**, 12 024 (1989).
3. A. H. Mahan, D. L. Williamson, B. P. Nelson, and R. S. Crandall, Solar Cells **27**, 465 (1989).
4. S. Guha and J. Yang, Appl. Phys. Lett. **61**, 1444 (1992).
5. P. J. Schultz and K. G. Lynn, Rev. Mod. Phys. **60**, 701 (1988).
6. S. Makinen and M. J. Puska, Phys. Rev. B **40**, 12 523 (1989).
7. R. N. West, Adv. Phys. **22**, 263 (1973).
8. K. G. Lynn, Phys. Rev. Lett. **43**, 391 (1979).
9. S. Dannefaer, D. Kerr, and B. G. Hogg, J. Appl. Phys. **54**, 155 (1983).
10. A. L. Jung, Y. H. Wang, G. Liu, J. J. Xiong, B. S. Cao, W. Z. Yu, and D. Adler, J. Non-Cryst. Solids **74**, 19 (1985).

11. A. L. Jung, Y. H. Wang, G. Lin, J. J. Xiong, B. S. Cao, W. Z. Yu, H. L. Jiang, J. Z. Song, K. Long, and D. Adler, J. Non-Cryst. Solids **77&78**, 221 (1985).
12. H. E. Schaefer, R. Würschum, R. Schwarz, D. Slobodin, and S. Wagner, Appl. Phys. A **40**, 145 (1986).
13. S. Dannefaer, P. Mascher, and D. Kerr, Appl. Phys. A **43**, 91 (1987).
14. H. E. Schaefer, R. Würschum, R. Schwarz, D. Slobodin, and S. Wagner, Appl. Phys. A **43**, 295 (1987).
15. P. H. Leo, K. D. Moore, P. L. Jones, and F. H. Cocks, Phys. Status Solidi B **108**, K145 (1981).
16. R. A. Hakvoort, S. Roorda, A. van Veen, M. J. van den Boogaard, F. J. M. Buters, and H. Schut, in *Positron Annihilation*, Proceedings of the 9th International Conference on Positron Annihilation, Szombathely, Hungary, August 26–31, 1991, edited by Zs. Kajcsos and Cs. Szeles (Trans Tech Publications, Switzerland, 1992), Vols. 105–107, p. 1391.
17. Xuanying Lin, Kuixun Lin, Yunpeng Yu, Y. W. Lam, Y. C. Chan, S. Lin, and F. Y. M. Chan, *Proceeding of First World Conference of Photovoltaic Energy Conversion*, Hawaii, December 5–9, 1994, p. 638.
18. C. D. Beling, S. Fung, H. M. Weng, C. V. Reddy, S. W. Fan, Y. Y. Shan, and C. C. Ling, American Institute of Physics, Conference Proceedings Series **303**, 462 (1994).
19. A. P. Mills, and R. Wilson, Phys. Rev. A **26**, 490 (1982).
20. J. Keinonen, M. Hautala, E. Rauhala, M. Erola, J. Lahtinen, H. Huomo, A. Vehanen, and P. Hautojärvi, Phys. Rev. B **36**, 1344 (1987).
21. A. Vehanen, K. Saarinen, P. Hautojärvi, and H. Huomo, Phys. Rev. B **35** 4606 (1987).
22. A. van Veen, H. Schut, R. A. J. de Vries, R. A. Hakvoort, and M. R. Ijpma, in *Positron Beams for Solid and Surfaces*, edited by P. J. Schultz, G. R. Massoumi, and P. J. Simpson (AIP Conference Proceeding, New York, 1991), Vol. 218, p. 171.
23. W. Luft and Y. S. Tsuo, *Hydrogenated Amorphous Silicon Alloy Deposition Processes* (Marcel Dekker, Inc., New York, Basel, Hong Kong, 1993), p. 15.
24. S. Dannefaer, G. W. Dean, D. P. Kerr, and B. G. Hogg, Phys. Rev. B **14**, 2709 (1976).
25. E. Soininen, J. Mäkinen, D. Beyer, and P. Hautojärvi, Phys. Rev. B **46**, 13 104 (1992).
26. S. Mantl and W. Triftschäuser, Phys, Rev. Lett. **48**, 1741 (1982).
27. S. Mantl and W. Triftschäuser, Phys. Rev. B **17**, 1645 (1978).
28. L. Liszkay, C. Corbel, L. Baroux, P. Hautojärvi, M. Bayhan, A. W. Brinkman, and S. Tatarenko, Appl. Phys. Lett. **64**, 1380 (1994).